Research on a Linear Direct-Current Plasma Accelerator

A. F. Carter,* G. P. Wood,† D. R. McFarland,‡ and W. R. Weaver*
NASA Langley Rearch Center, Hampton, Va.

Some results from a continuing research program on linear d.c. plasma accelerators are reported for an accelerator that has a channel 1 in. square and 12 in. long. This accelerator uses nitrogen seeded with 0.3% mole fraction cesium and operates at relatively high pressure, 50 mm Hg, and high magnetic field, 11,500 gauss. Power input to the accelerator is about 360 kw, with about 50 amp through each of 24 electrode pairs. The 1200-v axial potential difference, which is self-generated in the plasma between the ends of the accelerator, has posed operational problems, since this high voltage tends to find closed circuits to ground and back through paths external to the channel. Steps taken to alleviate these problems are described. Experience with the problem of erosion is described. A method for making time-of-flight velocity measurements, with an injected spark and an image-converter framing camera, has been developed. These measurements show an entrance velocity of 2000 m/sec and exit velocities of 6000–6850 m/sec. This tripling of the velocity by the accelerator is the best performance reported for an accelerator at rather high gas density, in this case 1.7×10^{-3} kg/m^3 at the exit.

Nomenclature§

a = speed of sound, m/sec
B = magnetic induction, webers/m^2
e = charge on singly charged positive ion, coul
E = electric field strength, v/m
h = enthalpy, joules/kg
j = current density, amp/m^2
l = distance across accelerator channel perpendicular to B field, m
$\dot{m}$ = mass flow rate, kg/s
M = Mach number, u/a
n = number density, m^{-3}
p = pressure, newtons/m^2
T = temperature, °K
u = velocity, m/sec
V = potential difference, v
x = coordinate in axial direction, m
y = coordinate normal to axis and applied B, m
z = coordinate in direction of applied B, m
ρ = mass density, kg/m^3
σ = scalar electrical conductivity, mho/m
τ = electron mean free time, sec
ω = electron cyclotron frequency, sec^{-1}

Subscripts

e = electron
P = pitot
t = total, stagnation
x = component in x direction
y = component in y direction
z = component in z direction

1. Introduction

THE current research program on d.c. linear crossed-field plasma accelerators at the Langley Research Center has as its primary objective the acquisition of data and experience to be used in the design and the development of a high-speed facility for investigation of re-entry problems, with reasonable simulation of velocity and density. Another objective is the obtaining of results that would be applicable to possible future space-ship propulsion systems. At the present stage of development of accelerators, the problems involved in improving their performance appear to be common to both applications. This paper describes the progress made with the accelerator currently used at Langley.

2. One-Inch-Square Accelerator Test Facility

A photograph of the accelerator installation is shown in Fig. 1. The seeding apparatus is at the far left. The arc heater is at the left, but is hardly visible. The accelerator is mounted in the large rectangular stainless-steel test chamber, about half of which extends from between the coils of the magnet, and which is connected at its right-hand end to a two-stage steam-ejector pump not shown in the photograph. Movie and television cameras are shown that look into the downstream end of the test chamber. A portion of the velocity-measuring apparatus is above the test chamber. Recording oscillographs are used for recording data. Currents, however, are measured by ammeters that are photographed by movie cameras. The use of ammeters was necessary because of high-voltage problems as discussed in Sec. 5. Four motor-generator sets in parallel, capable of supplying 4000 amp at 600 v, are available to power the arc heater. The accelerator is powered by batteries, each set of electrodes having its own separate supply.

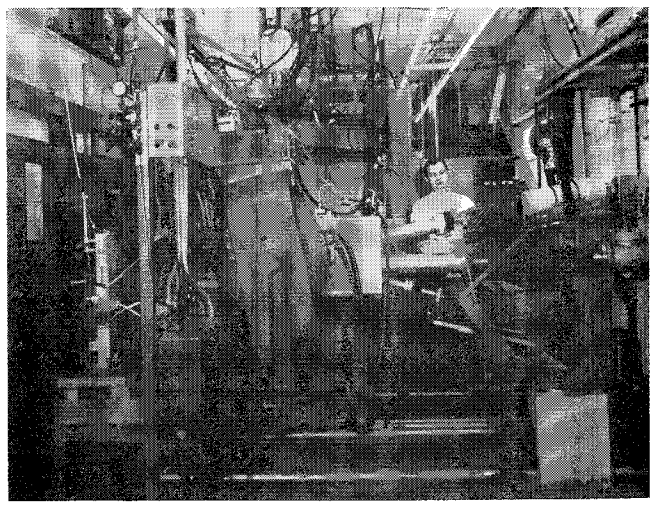

Fig. 1 One-inch-square accelerator installation.

Presented as Preprint 64-699 at the AIAA Fourth Electric Propulsion Conference, Philadelphia, Pa., August 31–September 2, 1964; revision received February 25, 1965.

* Aerospace Engineer.

† Head, Magnetohydrodynamics Section. Associate Fellow Member AIAA.

‡ Aerospace Engineer. Member AIAA.

§ Rationalized mksck system of units.

3. Arc Heater

The arc heater is a NASA design that was modified for use in this facility. A schematic is shown in Fig. 2. The water-cooled electrodes are axially symmetric, the outer one being the cathode and the inner one the anode. This arc heater does not give enthalpies high enough for the accelerator to operate without seeding. It was felt that seeding along the axis through the inner electrode would give better mixing than seeding through the sidewall; therefore, provision for seeding was made through the inner electrode as shown in Fig. 2. A large solenoid is used around the arc heater to spin the discharge. In the initial efforts to operate the arc heater, the discharge was very unstable and tended to be blown out by the aerodynamic force of the gas flow. Therefore, it was decided to reverse the current in one of the pancakes making up the solenoid to get a magnetic field distribution as shown in Fig. 2. It was hoped that a force, equal and opposite in direction to the aerodynamic force, would be generated from the operation of the arc in the gradient of a magnetic field. After the change in the field was made and the best axial location of the inner electrode with respect to the magnetic field gradient was determined, the arc operated in a stable position, indicating that a balance of forces had been achieved.

When attempts were made to operate the arc with seeding, however, more difficulties were experienced. When cesium vapor came into the arc heater, the arc voltage would drop from the normal operating value of 180 v to approximately 50 v. Since the amperage for either voltage is limited to about 2500 by the electrode design, this decrease in voltage causes a severe decrease in power input. Also, electrical breakdown to the end of the seeding tube was frequently experienced. These two problems were cured by a combination of three things. First, the seeding rate was reduced from 2% to 0.3 of 1%. A flow of 0.2 g/sec of nitrogen gas was introduced around the seeding tube in the space between it and the inner electrode. (This is only about 3% of the total nitrogen flow rate.) Also, all of the silver-soldered joints were eliminated on the end of the inner electrode in the vicinity of the seeding tube and replaced by copper weld joints. The arc heater then operated satisfactorily with seeding.

Some additional work was necessary, however, on the seeding tube itself. A 0.125-in.-o.d., 0.062-in.-i.d. stainless-steel tube 60 in. long, operated red hot, is used to vaporize the cesium. This tube, including the tip, must be maintained at a temperature greater than the boiling point of cesium; otherwise condensation will occur and the cesium will go into the arc heater in spurts. A stainless-steel tip was first used, but it was found that radiation from the hot plasma in the arc heater would melt it. In the limited space available, water cooling of the tip (to maintain its temperature between the boiling point of cesium and the melting point of the stainless steel) was attempted, but the temperature difference was found to be too small to accomplish this satisfactorily. Molybdenum was then used in place of the stainless steel, and melting of the tip was thus prevented. Satisfactory operation of the arc heater and the seeding tube together was then achieved. A drawing of the seeding tube is shown in Fig. 3.

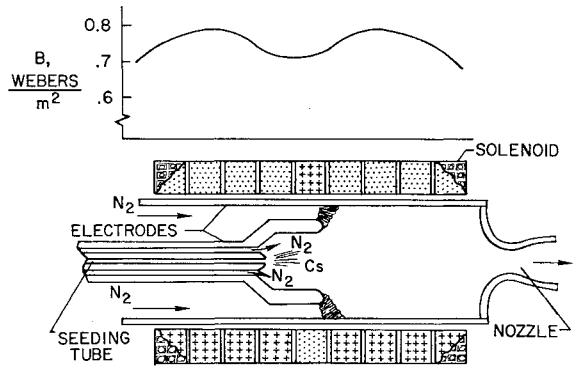

Fig. 2 Schematic diagram of arc heater and variation o magnetic induction.

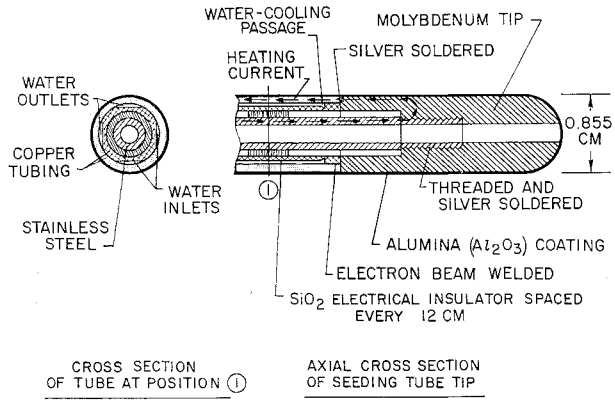

Fig. 3 Design of seeding tube.

4. Accelerator

The accelerator has a channel 1 in. × 1 in. in cross section and is 12 in. long. There are 24 pairs of electrodes; each electrode extends 0.285 in. in the axial direction. Insulators between electrodes extend 0.160 in. Electrodes have a transverse width of 1.75 in., of which 1 in. is exposed to the plasma. The anodes are tungsten of $\frac{1}{4}$-in. thickness which originally were backed by graphite but at present by copper for better electrical contact and better heat transfer. For the same applied voltage between anode and cathode, nearly the same current is obtained whether the cathodes are tungsten or thoriated tungsten, whether they are $\frac{1}{16}$-or $\frac{1}{8}$-in. thick, or whether they are backed by graphite or copper for $\frac{3}{8}$ in. at each end. The insulators between the electrodes are boron nitride, as are the sidewalls. A picture of the assembled accelerator is shown in Fig. 4. The accelerator is shown with one sidewall removed in Fig. 5.

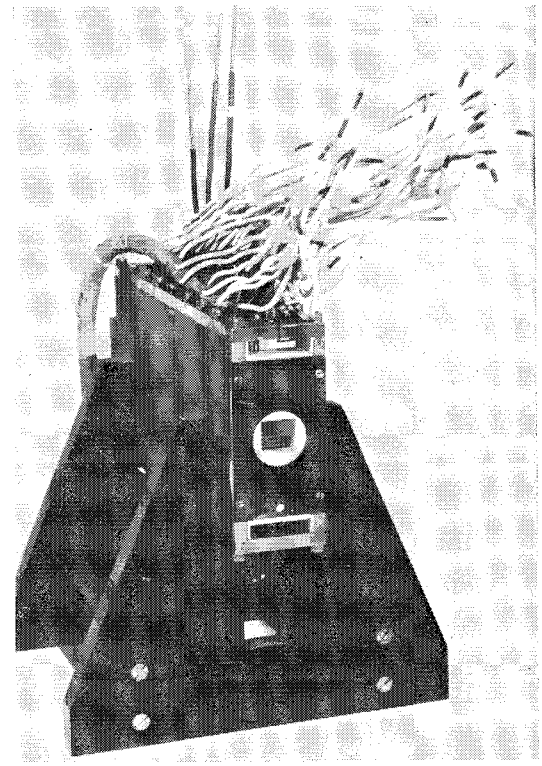

Fig. 4 Assembled 1-in.-square accelerator.

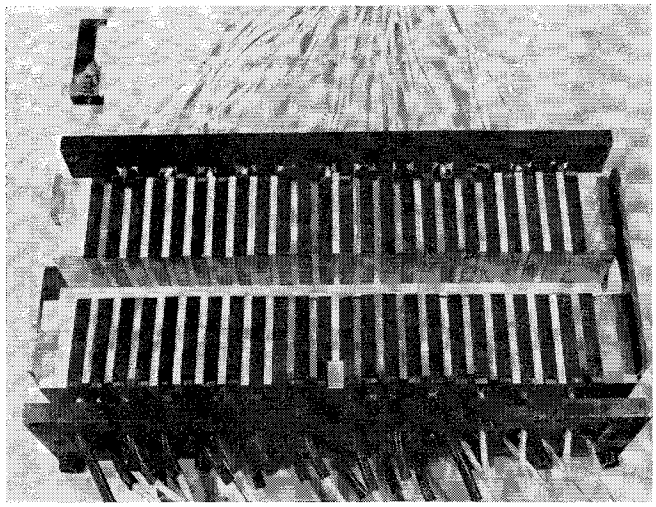

Fig. 5 Accelerator with sidewall removed.

5. Applied, Hall, and Sheath Potential Differences

Figure 6 shows a typical distribution of the applied voltage and the amperage in the accelerator. The voltage distribution along the accelerator channel has been adjusted to result in approximately constant-current operation. The average current through each electrode is seen to be approximately 55 amp, whereas the average voltage is about 275 v.

Figure 7 shows a plot of the axial potential along the accelerator. This is the potential variation developed by the plasma, since no V_x is applied to the electrodes. The value of E_x, as determined from these measurements, is 5100 v/m. It should be noted that the value of E_x is constant over the accelerator length. A simple expression for E_x can be derived by writing Ohm's law for the current density in the axial direction and setting it equal to zero

$$i_x = \sigma(E_x - u_{e,y}B_z) = 0$$

or

$$E_x = u_{e,y}B_z$$

and since

$$j_y \approx n_e e u_{e,y}$$

then

$$E_x \approx j_y B_z / n_e e$$

The quantities j_y, B_z, and E_x can be determined readily from measurements, and therefore n_e, the number density of electrons, can be obtained. For the test in which the data of Fig. 7 were obtained, j_y was 1.6×10^5 amp/m^2, and B was 1.14 webers/m^2. With these values, then, n_e was 2.3×10^{20} electrons/m^3.

Electron number density can also be calculated from the known mass flow rate, the measured velocity, and the seed mole fraction of original undissociated nitrogen. At the entrance to the accelerator, the value obtained by this method is 3.3×10^{20} electrons/m^3. This value of n_e is larger than the value obtained by using the measured value of E_x in the accelerator. There is, however, always condensation of some of the cesium vapor in the arc-heater plenum and nozzle sections, and this may result in the actual value of n_e being less than the value calculated by this method.

A subsequent section shows that the velocity of the plasma is increased by a factor of 3. Therefore, the electron density of the seeded gas would be expected to be reduced by the same factor, since the channel is of constant cross-sectional area. In the expression for E_x, j_y and B are constant; therefore, E_x would be expected to be larger at the accelerator exit by a factor of 3. However, E_x is seen to be constant over most of the accelerator length. It must be concluded that there are additional electrons other than those formed from ionization of the seeding material and that they are produced at a rate such that the total number density of electrons remains approximately constant along the accelerator channel. The additional ionization probably comes from the nitrogen, but a calculation of the required temperature shows that the neutral gas temperature cannot be high enough to produce this ionization, and that, therefore, an elevated electron temperature must be responsible. It can be shown that the additional electron density can be provided if the electron temperature is only about $\frac{1}{4}$ higher than the gas temperature. This is within the range that might be expected.

A calculation of the value of the scalar conductivity, using the number density obtained from E_x, gives 410 mho/m at the entrance and 1200 at the exit. When the effective (due to electrode widths greater than infinitesimal, and to the large $\omega\tau$ of about 16) value of conductivity is calculated by the method of Ref. 1, the value is found to be about 40 mho/m at the entrance and 80 at the exit.

The voltage difference required across the channel, which is given by

$$V_y = l(j_y/\sigma + u_x B_z)$$

is 170 v at the entrance to the accelerator and 235 v at the exit. The combined drop at the anode and cathode near the accelerator entrance is, therefore, approximately 105 v and at the accelerator exit approximately 40 v.

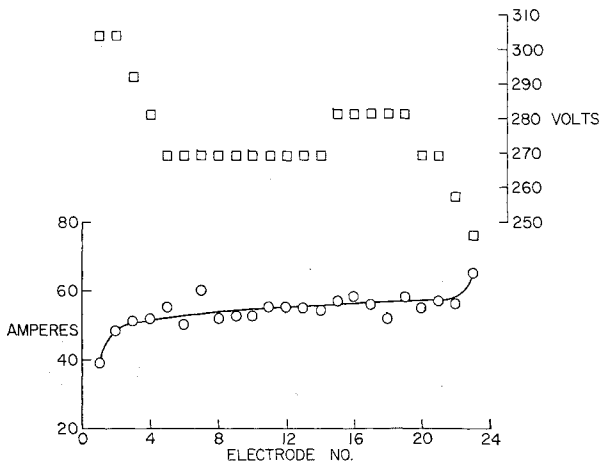

Fig. 6 Currents and applied voltages across accelerator.

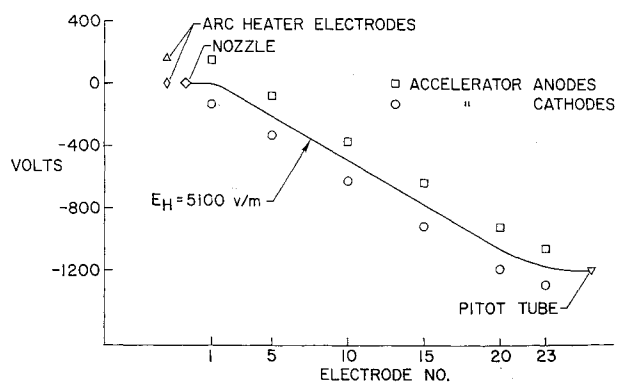

Fig. 7 Potential distribution in arc heater, nozzle, and accelerator.

The axial potential difference developed in the accelerator created some troublesome problems during the efforts to make the accelerator operational. The 48 leads to the accelerator electrodes were fed through a metal plate (the lid to the test chamber) and ceramic-insulated terminals were soldered into it for electrical feedthroughs. When the accelerator was turned on, electrical breakdown occurred inside the test chamber at the lid where the current-carrying conductors came through it. The problem was solved by bringing teflon-insulated wires through the cover of the test chamber without breaking the insulation until the wires were connected to the accelerator. A small O ring was used around each wire to provide a leak-free seal.

Additional problems were experienced with the instrumentation because of the axial potential gradient. Three recorders used to record the test data were insulated for only 600 v from galvanometer elements to the case, or ground. Burnout of the galvanometer elements and then arc-over to the case occurred at the elements that measured currents through electrical shunts in the leads to the upstream electrodes. The plasma at the downstream end of the accelerator grounds itself to the test chamber to form the return current path. Therefore, all currents were measured by using panel ammeters photographed by movie cameras, and two of the recorders were disconnected. The high voltage then found its way to ground by breaking down in the meter that measures arc current. This meter and the meter-measuring arc voltage were then mounted on a large dielectric plate to insure complete isolation. By measuring all voltages and currents on panel-type meters photographed by movie cameras and by using the recorders to measure only temperatures and pressures, many successful operations of the accelerator have been achieved; the results from some of them are reported in this paper and some are reported elsewhere.[2]

Trouble was eventually experienced with the motor-generator sets that power the arc heater. Operation at 1200 to 1500 v above ground potential was suspected to have caused the difficulty. The motor-generator sets could be grounded through a suitable resistance if the downstream end of the accelerator could be isolated so that the potential there could go to 1200 to 1500 v negative. To isolate the test chamber from ground, a dielectric plate was inserted in the upstream support pedestal, and a 20-in.-long section of dielectric pipe was inserted in the pipe leading from the test chamber to the vacuum pump. This failed to provide sufficient isolation, because breakdown to ground occurred in the gas flowing through the insulating pipe, allowing axial current flow in the accelerator. Steam was then sprayed into the pipe downstream of the test chamber to quench the ionization. This prohibited breakdown from occurring and operation of the accelerator was then quite satisfactory. The data in Fig. 7 were taken from a run after isolation of the test chamber was accomplished.

6. Erosion

The present 1-in.-square accelerator is not water-cooled, and therefore test durations are limited because of the large power input and the small heat capacity of the accelerator. The limit on duration is approximately 3 sec, because the anodes reach high temperatures quickly. A photograph of the anode wall using $\frac{1}{16}$-in.-thick tungsten for the electrodes is shown in Fig. 8. When $\frac{1}{4}$-in.-thick tungsten is used for anodes, the melting is almost completely eliminated for the test time of 3 sec, as is shown in Fig. 9. Considerable erosion of the boron nitride sidewalls occurred, even though they were stored under vacuum and at temperatures of 250°F. However, a new grade of boron nitride is now available which has an erosion resistance much superior to the former grade of material. The erosion is virtually eliminated if the boron nitride is used within four to six weeks after being removed from moisture-proof containers and stored at atmospheric conditions. Figure 10 shows a photograph of used channel sidewalls made from boron nitride and from the new grade of boron nitride used within the four- to six-week period.

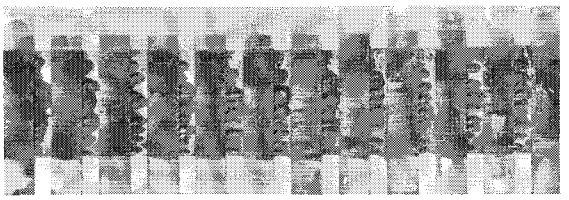

Fig. 9 Erosion of $\frac{1}{4}$-in.-thick anodes.

7. Diagnostics

Since the 1-in.-square accelerator became operational, the primary effort has been to develop a direct method of velocity measurement, inasmuch as velocity is the parameter of greatest interest. The apparatus and its functioning are described here in some detail, because the method appears to give excellent results. The early attempts to measure velocity were made at the exit of the nozzle of the arc heater to establish firmly the conditions existing there. The method consisted of creating a region of high luminosity by injecting a spark across the flow emerging from the nozzle and using two photomultiplier tubes located downstream of the injection point to detect the luminosity in the flow as it passed. A dual-beam oscilloscope recorded the passage of the luminous pulses. This method had the disadvantage that the isolation of the high voltage necessary to obtain a rather energetic spark was somewhat of a nuisance. Secondly, the luminosity from the spark had become rather diffuse by the time it reached the downstream photomultiplier. The first of these difficulties was overcome by proper selection of components, but the second could never be completely overcome satisfactorily. Nevertheless, reasonably good measurements were obtained.

The next step was to extend the technique to measuring velocities at the accelerator exit. It was felt that, instead of monitoring the motion of the luminosity with photomultiplier tubes, pictures of the spark could be taken as it moved

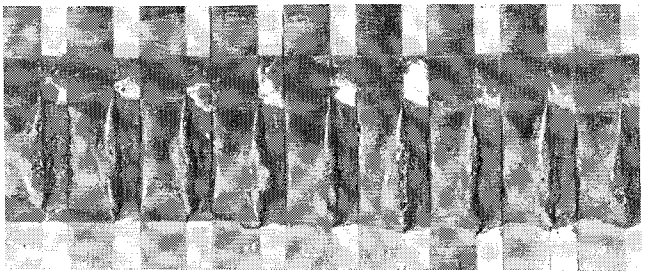

Fig. 8 Erosion of $\frac{1}{16}$-in.-thick anodes.

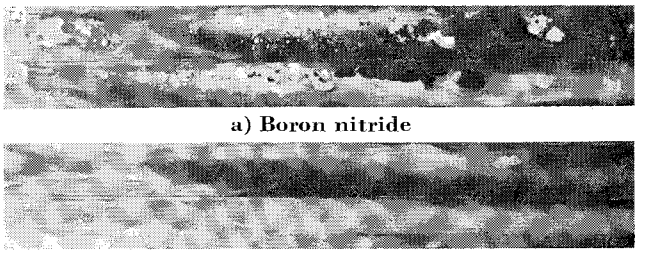

a) Boron nitride

b) New improved boron nitride

Fig. 10 Erosion of sidewalls.

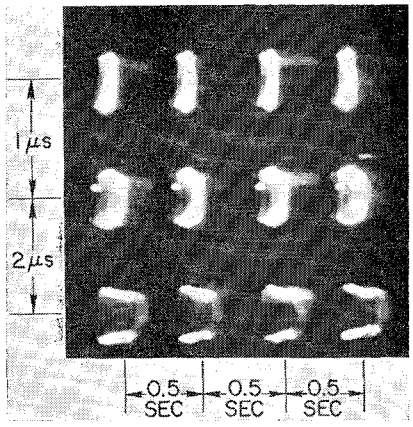

Fig. 11 Image-converter camera pictures of luminous gas from spark.

downstream by using an image-converter camera. Measurement of the displacement over a given time interval could then be used to obtain the velocity. The camera that was used takes three frames in sequence, with variable exposure times and variable time between exposures. To increase the probability of obtaining usable data, the film holder was motorized, and a series of six sequences were taken for each 3-sec run, each sequence containing three frames. Figure 11 shows a series of four sequences with the accelerator on. The method of taking the pictures follows a set procedure. A motorized cam is used to actuate a switch six times, once every $\frac{1}{2}$ sec. The cam-driving motor is energized when the accelerator is turned on. Each time the switch closes, the mechanical shutter on the image converter camera is opened. The switch also starts a time-delay circuit that triggers the spark discharge through a triggered spark gap after the mechanical shutter has had time to open fully. The camera has an electronic shutter, but use of the mechanical shutter is necessary because of the strong light intensity from the plasma, and the fact that the electronic shutter has a transmission ratio as large as 1 to 10^6. Just as much light would reach the film if the mechanical shutter were open for 0.2 sec, with the electronic shutter closed as it reaches it during the 0.2-μsec exposure with the electronic shutter. The mechanical shutter was set for $\frac{1}{2}$ sec, and good pictures were obtained. The electronic shutter is actuated by a signal obtained by inductive coupling through a one-turn loop around one of the leads to the spark discharge. The three-frame sequence is then automatic.

A word of caution may be in order. Care must be taken that the current has decayed before the current path has swept downstream of the electrodes. Otherwise, the possibility of rail-type acceleration of the spark would exist. For the data presented in this paper, the current was damped to practically zero in less than 1 μsec, or before the second frame was taken, by proper choice of voltage and capacitance and by inserting a 3-ohm damping resistance in series with the discharge. It is therefore believed that the current approached zero before any significant deviation occurred in the current path from a straight line between the electrodes.

Various values of voltage and capacitance were used in these experiments to arrive at a system giving good results. The following is a description of the spark discharge circuit that was finally adopted. A 50-kv, 0.02-μf capacitor is charged to approximately 30 kv. A 50-kv triggered spark gap and a 3-ohm damping resistance are included in the circuit. Teflon-insulated wires are fed through the dielectric lid of the test chamber without breaking the insulation. Small O rings provide a leak-free seal. The two leads are soldered to a piece of $\frac{1}{8}$-in., hard copper tubing and then an alumina tube is slipped over the copper tubing and extends up over the teflon insulation for approximately 3 in. A $\frac{1}{16}$-in.-diam hole is drilled into the side of each alumina tube and into the copper. Tungsten wires for the spark electrodes $\frac{1}{16}$ in. in diameter are then inserted into the holes and held in place with set screws threaded into the end of the copper tubing. This has worked very well in keeping the high-voltage spark from breaking down to undesired places.

In addition to velocity measurements, measurements of the pitot pressure at the exit of the accelerator are made. Measurements of pitot pressure and observations with a movie camera of the bow shock wave are made with the end of the pitot tube about 0.25 in. from the exit of the accelerator. This location was used to assure that the end of the pitot tube would be inside any expansion or shock waves formed at the exit. Observation of the bow-shock wave for both accelerator on-and-off conditions can be used to verify that the flow is supersonic. The shock standoff distance from the end of the pitot tube is also observed. Figure 12 shows the shape and location of the bow shock at the pitot tube for the accelerator off-and-on conditions. The fact that the standoff distance decreases when the accelerator is turned on indicates an increase in the Mach number of the flow.

8. Results

The conditions at the exit of the supersonic nozzle (and therefore at the entrance to the accelerator) have been determined by a long series of experiments with the accelerator removed from the test chamber. The following is a list of representative values for the state of the gas: $\dot{m} = 6.68 \times 10^{-3}$ kg/sec, $h = 6.2 \times 10^6$ joules/kg, $h_t = 8.2 \times 10^6$ joules/kg, $p = 6.9 \times 10^3$ newtons/m^2, $u = 2.0 \times 10^3$ m/sec, $\rho = 5.2 \times 10^{-3}$ kg/m^3, $T = 4.4 \times 10^3$ °K, $p_P = 1.7 \times 10^4$ newtons/m^2, $a = 1.24 \times 10^3$ m/sec, and $M = 1.6$.

The results of measurements of velocity at the exit of the accelerator during various runs show velocities between 6000 and 6850 m/sec with uncertainties of about 8%. The uncertainties were determined by having several persons make independent determinations of the velocity from the photographs and from measurements made between the various frames in a given sequence. The increase in velocity obtained with this accelerator (an acceleration from 2000 to 6000 m/sec or more) is by far the largest that has been reported for a linear plasma accelerator that operates at the reasonably high density level of this one.

The electrical power input into the arc heater and into the accelerator were measured for each run. The energy in the gas at the accelerator entrance is known from measurement of the energy loss to the cooling water of the arc heater and the nozzle. If the voltage drops estimated at the electrode sheaths are considered, then the energy added to the gas stream can be determined approximately. At the accelerator entrance, $h = 0.6 \times 10^7$ joules/kg and $u^2/2 = 0.20 \times 10^7$ joules/kg. The accelerator adds $\Delta h = 1.6 \times 10^7$ joules/kg and $\Delta(u^2/2) = 1.6 \times 10^7$ joules/kg. At the accelerator exit, $h = 2.2 \times 10^7$ joules/kg and $u^2/2 = 1.8 \times 10^7$ joules/kg. The calculated thrust of the accelerator is 20 newtons (4.5 lb).

Typical values of the pitot pressure at the exit are 2.1×10^4 newtons/m^2 (0.21 atm) with the accelerator turned off

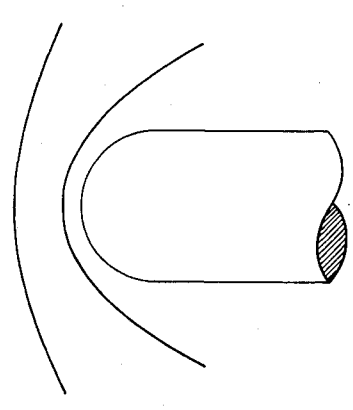

Fig. 12 Bow-shock waves with accelerator off and on (from photographs).

and 7.6×10^4 newtons/m^2 (0.75 atm) when the accelerator is operating.

9. Future Accelerators

The present accelerator, although its operation is limited in duration to about 3 sec, serves well during this phase of the research program. To overcome the disadvantage of such short running time, a water-cooled version of it has been designed and constructed.

A larger accelerator has also been designed to give an exit velocity of 12,000 m/sec at a density of 3×10^{-4} kg/m^3. The accelerator will have a channel of 2.5- $\times$ 2.5-in. cross section and will be 18 in. long. It will be operated from a 10-Mw d.c. supply, and a second 10-Mw d.c. supply will power the arc heater.

References

[1] Hurwitz, H., Jr., Kilb, R. W., and Sutton, G. W., "Influence of tensor conductivity on current distribution in a MHD generator," J. Appl. Phys. **32**, 205–216 (1961).

[2] Wood, G. P., Carter, A. F., Sabol, A. P., McFarland, D. R., and Weaver, W. R., "Research on linear crossed-field steady-flow D-C plasma accelerators at Langley Research Center, NASA," AGARD Specialists' Meeting on Arc Heaters and MHD Accelerators for Aerodynamic Purposes, AGARDograph 84 (September 21–23, 1964).

JUNE 1965 AIAA JOURNAL VOL. 3, NO. 6

Energy Loss in Pulsed Coaxial Plasma Guns

D. E. T. F. Ashby*
General Dynamics/Convair, San Diego, Calif.

The one-dimensional flow of a current-carrying plasma, driven into neutral gas by its self-magnetic field, is considered for the case where both the neutral gas and the current have arbitrary distributions in the direction of flow. The conservation laws are used to derive a simple expression for the amount of input power that goes into all forms of internal energy. It is shown that this power depends mainly on the rate at which the current sheet sweeps up neutral gas. In principle, internal energy can be converted into directed energy by expansion; however, it is argued that, in the coaxial plasma accelerators currently used in propulsion studies, most of the internal energy will be lost by excitation and subsequent radiation or ionization before expansion occurs.

I. Introduction

TWO simple models are commonly used to describe the operation of coaxial guns.[1] The "slug model"[2] assumes that a plasma of constant mass is accelerated into a vacuum, whereas the "shock model"[2, 3] assumes that the barrels are uniformly filled with neutral gas that is ionized and accelerated by a shock driven by the $j \times B$ forces. The conservation laws show that, when a shock moves with constant velocity into a stationary gas, half of the energy supplied to the plasma appears in directed motion, whereas the other half is taken by internal energy of one form or another; the slug model, however, avoids this energy loss. In a real accelerator, the gas distribution will lie between the extremes described by the two models.

This paper has two objectives; firstly to obtain a general expression for the energy loss that occurs when the gas distribution ahead of the current sheet is arbitrary and secondly to consider the implications of this expression for the coaxial guns currently used to investigate the problems of pulsed plasma propulsion.

II. Theory†

A one-dimensional model with plane electrodes is considered (Fig. 1). It is assumed that all quantities vary only in the z direction and with time. The main variables are

$\mathbf{B} = [0, B(z), 0]$ = magnetic flux density
$\mathbf{u} = [0, 0, u(z)]$ = fluid velocity
$p(z)$ = fluid pressure
$\rho(z)$ = fluid density

Two planes in the xy plane are defined. The first plane at $z = z_1$ moves with velocity v_1 and marks the boundary between magnetic field plus plasma and magnetic field alone; it will be referred to as the piston. Because no plasma flows through this plane, $u_1 = v_1$. The second plane at $z = z_2$ moves with velocity v_2 and marks the boundary between the initial stationary gas and gas that has been affected by the moving piston. Electric currents and plasma motion are restricted to the region between planes 1 and 2.

The conservation laws may be written as follows:

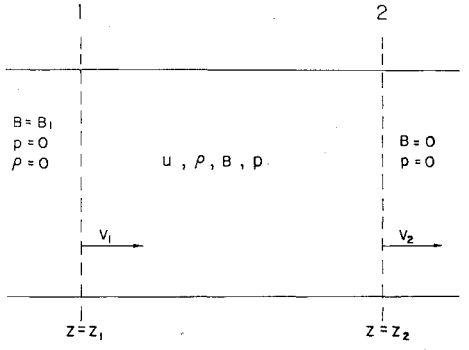

Fig. 1 Diagram illustrating the theoretical model

Received October 13, 1964; revision received March 22, 1965. This work was supported by NASA under Contract No. NAS3-2594.

* Consultant; on leave of absence from Culham Laboratory, Berkshire, England.

† Based on an analysis in Ref. 4.